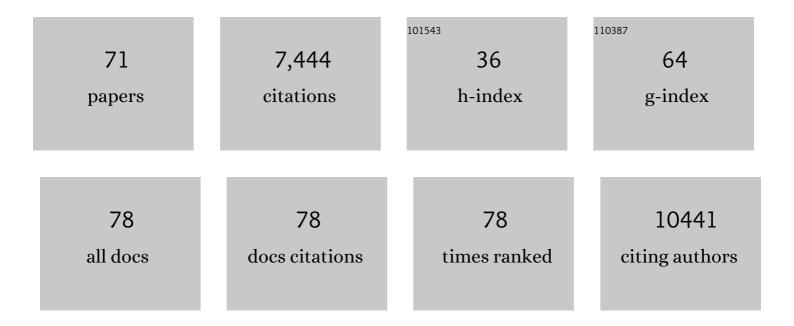
## Gunnar F. SchrĶder

List of Publications by Year in descending order

Source: https://exaly.com/author-pdf/8044498/publications.pdf

Version: 2024-02-01



CHNNAD F SCHDÃIDED

#	Article	IF	CITATIONS
1	Major tail proteins of bacteriophages of the order Caudovirales. Journal of Biological Chemistry, 2022, 298, 101472.	3.4	37
2	High-Resolution Cryo-EM Structure of the Cardiac Actomyosin Complex. Structure, 2021, 29, 50-60.e4.	3.3	41
3	Cryo-EM model validation recommendations based on outcomes of the 2019 EMDataResource challenge. Nature Methods, 2021, 18, 156-164.	19.0	73
4	Clustering polymorphs of tau and IAPP fibrils with the CHEP algorithm. Progress in Biophysics and Molecular Biology, 2021, 160, 16-25.	2.9	10
5	Amyloid-type Protein Aggregation and Prion-like Properties of Amyloids. Chemical Reviews, 2021, 121, 8285-8307.	47.7	98
6	Endo-lysosomal Aβ concentration and pH trigger formation of Aβ oligomers that potently induce Tau missorting. Nature Communications, 2021, 12, 4634.	12.8	59
7	Challenges in sample preparation and structure determination of amyloids by cryo-EM. Journal of Biological Chemistry, 2021, 297, 100938.	3.4	20
8	The <i>Uppsala APP</i> deletion causes early onset autosomal dominant Alzheimer's disease by altering APP processing and increasing amyloid β fibril formation. Science Translational Medicine, 2021, 13, .	12.4	23
9	Conformational heterogeneity coupled with β-fibril formation of a scaffold protein involved in chronic mental illnesses. Translational Psychiatry, 2021, 11, 639.	4.8	9
10	Engineering and application of a biosensor with focused ligand specificity. Nature Communications, 2020, 11, 4851.	12.8	56
11	Atomistic structure and dynamics of the human MHC-I peptide-loading complex. Proceedings of the National Academy of Sciences of the United States of America, 2020, 117, 20597-20606.	7.1	40
12	Architecture of the flexible tail tube of bacteriophage SPP1. Nature Communications, 2020, 11, 5759.	12.8	37
13	Cryo-EM structure of islet amyloid polypeptide fibrils reveals similarities with amyloid-β fibrils. Nature Structural and Molecular Biology, 2020, 27, 660-667.	8.2	120
14	Integrating cryo-EM and NMR data. Current Opinion in Structural Biology, 2020, 61, 173-181.	5.7	23
15	Atomic structure of PI3-kinase SH3 amyloid fibrils by cryo-electron microscopy. Nature Communications, 2019, 10, 3754.	12.8	32
16	α-Synuclein-derived lipoparticles in the study of α-Synuclein amyloid fibril formation. Chemistry and Physics of Lipids, 2019, 220, 57-65.	3.2	9
17	Integrated NMR, Fluorescence, and Molecular Dynamics Benchmark Study of Protein Mechanics and Hydrodynamics. Journal of Physical Chemistry B, 2019, 123, 1453-1480.	2.6	29
18	Clustering cryo-EM images of helical protein polymers for helical reconstructions. Ultramicroscopy, 2019, 203, 132-138.	1.9	9

Gunnar F. SchrĶder

#	Article	IF	CITATIONS
19	N-Terminal Domains of Cardiac Myosin Binding Protein C Cooperatively Activate the Thin Filament. Structure, 2018, 26, 1604-1611.e4.	3.3	57
20	Ca <sup>2+</sup> -induced movement of tropomyosin on native cardiac thin filaments revealed by cryoelectron microscopy. Proceedings of the National Academy of Sciences of the United States of America, 2017, 114, 6782-6787.	7.1	63
21	Conformational Heterogeneity in a Fully Complementary DNA Three-Way Junction with a GC-Rich Branchpoint. Biochemistry, 2017, 56, 4985-4991.	2.5	12
22	Fibril structure of amyloid-β(1–42) by cryo–electron microscopy. Science, 2017, 358, 116-119.	12.6	801
23	Protein structure refinement with adaptively restrained homologous replicas. Proteins: Structure, Function and Bioinformatics, 2016, 84, 302-313.	2.6	10
24	Archaeal flagellin combines a bacterial type IV pilin domain with an Ig-like domain. Proceedings of the National Academy of Sciences of the United States of America, 2016, 113, 10352-10357.	7.1	49
25	The pathway to GTPase activation of elongation factor SelB on the ribosome. Nature, 2016, 540, 80-85.	27.8	93
26	β-Hairpin of Islet Amyloid Polypeptide Bound to an Aggregation Inhibitor. Scientific Reports, 2016, 6, 33474.	3.3	34
27	Near-Atomic Resolution for One State of F-Actin. Structure, 2015, 23, 173-182.	3.3	121
28	Archaeal actin from a hyperthermophile forms a single-stranded filament. Proceedings of the National Academy of Sciences of the United States of America, 2015, 112, 9340-9345.	7.1	22
29	Improving the visualization of cryo-EM density reconstructions. Journal of Structural Biology, 2015, 191, 207-213.	2.8	17
30	Outcome of the First wwPDB Hybrid/Integrative Methods Task Force Workshop. Structure, 2015, 23, 1156-1167.	3.3	159
31	Hybrid methods for macromolecular structure determination: experiment with expectations. Current Opinion in Structural Biology, 2015, 31, 20-27.	5.7	37
32	Coupling an Ensemble of Homologues Improves Refinement of Protein Homology Models. Journal of Chemical Theory and Computation, 2015, 11, 5578-5582.	5.3	4
33	Deformable elastic network refinement for low-resolution macromolecular crystallography. Acta Crystallographica Section D: Biological Crystallography, 2014, 70, 2241-2255.	2.5	29
34	Unified Polymerization Mechanism for the Assembly of ASC-Dependent Inflammasomes. Cell, 2014, 156, 1193-1206.	28.9	1,035
35	Ligand-induced structural changes in the cyclic nucleotide-modulated potassium channel MloK1. Nature Communications, 2014, 5, 3106.	12.8	59
36	Rapid and Stable Transfer RNA Translocation through the Ribosome Ensured by Specific Contact Mechanisms. Biophysical Journal, 2014, 106, 493a.	0.5	0

Gunnar F. SchrĶder

#	Article	IF	CITATIONS
37	Ribosomal Kinetics and Concerted Motions from Nanoseconds to Seconds. Biophysical Journal, 2014, 106, 250a.	0.5	0
38	Cryo-Electron Microscopy of Potassium Channel Membrane Proteins. Microscopy and Microanalysis, 2014, 20, 1206-1207.	0.4	0
39	Mechanisms for Efficient TRNA Translocation through the Ribosome. Biophysical Journal, 2013, 104, 16a.	0.5	0
40	Energy barriers and driving forces in tRNA translocation through the ribosome. Nature Structural and Molecular Biology, 2013, 20, 1390-1396.	8.2	150
41	Structural Polymorphism of F-Actin is Coupled with its Mechanical Properties. Biophysical Journal, 2013, 104, 644a-645a.	0.5	0
42	Rate Estimates from Sampling Sparse Transitions: TRNA Motion Limits Transitions between Ribosomal Translocation Intermediates. Biophysical Journal, 2013, 104, 663a.	0.5	0
43	The Crystal Structures of the Eukaryotic Chaperonin CCT Reveal Its Functional Partitioning. Structure, 2013, 21, 540-549.	3.3	59
44	Visualizing GroEL/ES in the Act of Encapsulating a Folding Protein. Cell, 2013, 153, 1354-1365.	28.9	102
45	Cross-validation in cryo-EM–based structural modeling. Proceedings of the National Academy of Sciences of the United States of America, 2013, 110, 8930-8935.	7.1	42
46	Small-angle X-ray Scattering of Apolipoprotein A-IV Reveals the Importance of Its Termini for Structural Stability. Journal of Biological Chemistry, 2013, 288, 4854-4866.	3.4	10
47	Symmetry-free cryo-EM structures of the chaperonin TRiC along its ATPase-driven conformational cycle. EMBO Journal, 2012, 31, 720-730.	7.8	80
48	Remodeling of Actin Filaments by Cofilin. Biophysical Journal, 2012, 102, 238a.	0.5	0
49	Filaments from Ignicoccus hospitalis Show Diversity of Packing in Proteins Containing N-Terminal Type IV Pilin Helices. Journal of Molecular Biology, 2012, 422, 274-281.	4.2	40
50	Dynamic, Energetic, and Kinetic Determinants of Ribosomal Translocation: Microsecond All-Atom Simulations of Hybrid Cryoem/X-Ray Structural Substates. Biophysical Journal, 2012, 102, 67a.	0.5	0
51	Branchpoint Expansion in a Fully Complementary Three-Way DNA Junction. Journal of the American Chemical Society, 2012, 134, 6280-6285.	13.7	44
52	A grid-enabled web service for low-resolution crystal structure refinement. Acta Crystallographica Section D: Biological Crystallography, 2012, 68, 261-267.	2.5	17
53	Improving the Accuracy of Macromolecular Structure Refinement at 7ÂÃ Resolution. Structure, 2012, 20, 957-966.	3.3	37
54	Realâ€space refinement with DireX: From global fitting to sideâ€chain improvements. Biopolymers, 2012, 97, 687-697.	2.4	52

#	Article	IF	CITATIONS
55	Application of DEN refinement and automated model building to a difficult case of molecular-replacement phasing: the structure of a putative succinyl-diaminopimelate desuccinylase from <i>Corynebacterium glutamicum</i> . Acta Crystallographica Section D: Biological Crystallography, 2012, 68, 391-403.	2.5	26
56	Clobal Structure of Forked DNA in Solution Revealed by High-Resolution Single-Molecule FRET. Journal of the American Chemical Society, 2011, 133, 1188-1191.	13.7	36
57	Structure of Myxovirus Resistance Protein A Reveals Intra- and Intermolecular Domain Interactions Required for the Antiviral Function. Immunity, 2011, 35, 514-525.	14.3	188
58	Remodeling of actin filaments by ADF/cofilin proteins. Proceedings of the National Academy of Sciences of the United States of America, 2011, 108, 20568-20572.	7.1	194
59	The refined structure of functional unit h of keyhole limpet hemocyanin (KLH1â€h) reveals disulfide bridges. IUBMB Life, 2011, 63, 183-187.	3.4	23
60	A Spring-loaded Release Mechanism Regulates Domain Movement and Catalysis in Phosphoglycerate Kinase. Journal of Biological Chemistry, 2011, 286, 14040-14048.	3.4	53
61	Structural polymorphism in F-actin. Nature Structural and Molecular Biology, 2010, 17, 1318-1323.	8.2	170
62	Mechanism of folding chamber closure in a group II chaperonin. Nature, 2010, 463, 379-383.	27.8	196
63	Super-resolution biomolecular crystallography with low-resolution data. Nature, 2010, 464, 1218-1222.	27.8	267
64	Recognition Dynamics Up to Microseconds Revealed from an RDC-Derived Ubiquitin Ensemble in Solution. Science, 2008, 320, 1471-1475.	12.6	963
65	Single-molecule FRET measures bends and kinks in DNA. Proceedings of the National Academy of Sciences of the United States of America, 2008, 105, 18337-18342.	7.1	172
66	Combining Efficient Conformational Sampling with a Deformable Elastic Network Model Facilitates Structure Refinement at Low Resolution. Structure, 2007, 15, 1630-1641.	3.3	213
67	Detecting protein-induced folding of the U4 snRNA kink-turn by single-molecule multiparameter FRET measurements. Rna, 2005, 11, 1545-1554.	3.5	46
68	Simulation of Fluorescence Anisotropy Experiments: Probing Protein Dynamics. Biophysical Journal, 2005, 89, 3757-3770.	0.5	128
69	FRETsg: Biomolecular structure model building from multiple FRET experiments. Computer Physics Communications, 2004, 158, 150-157.	7.5	20
70	Maximum likelihood trajectories from single molecule fluorescence resonance energy transfer experiments. Journal of Chemical Physics, 2003, 119, 9920-9924.	3.0	62
71	Single-molecule fluorescence resonance energy transfer reveals a dynamic equilibrium between closed and open conformations of syntaxin 1. Proceedings of the National Academy of Sciences of the United States of America, 2003, 100, 15516-15521.	7.1	268